STRUCTURAL MONITORING AND DIAGNOSTICS BY THE ACOUSTIC EMISSION TECHNIQUE: SCALING OF DISSIPATED ENERGY IN COMPRESSION

Alberto Carpinteri, Giuseppe Lacidogna

Politecnico di Torino,
Department of Structural Engineering and Geotechnics,
Corso Duca degli Abruzzi 24 - 10129 Torino, Italy
carpinteri@polito.it

Abstract

The Acoustic Emission (AE) technique is applied to examine some aspects influencing concrete failure in compression. The homogeneity of the material and the amount of energy dissipated during the failure process of concrete specimens have been estimated. The experimental results show peculiar scale effects on these mechanical properties.

INTRODUCTION

Monitoring techniques are assuming an increasing importance in the evaluation of structural conditions and reliability. The nondestructive methodology based on AE, originally developed for industrial steel components, is nowadays being applied also in the field of civil structures [1].

By means of this technique, we have analyzed the evolution of cracks in a compressed concrete wall located in the basement of a building, and drilled some cylindrical specimens in order to detect the mechanical properties of the material at the laboratory scale. With this methodology, therefore, it is possible to evaluate the relations between diffused microcracking and coalescence of macrodefects in real structural elements. Scaling of the dissipated energy in compression is also considered.

FUNDAMENTALS OF AE TECHNIQUE

Cracking is accompanied by emission of elastic waves which propagate within bulk material. These waves can be received and recorded by transducers applied on the surface of the structural element [3]. The AE method, which is called Ring-Down Counting or Event-Counting, considers the number of waves beyond a certain threshold level and is widely used for defect analysis (Fig.1) [4,5]. As a first approximation, in fact, the cumulative number of counts N_T can be compared with the amount of energy released during the loading process, assuming that both quantities grow proportionally to the extent of damage. The quantity that characterises the distribution of peak amplitude is the cumulative distribution $N(v)$, which represents the number of recorded signals with peak amplitude larger than v (measured in Volt). Similar analyses are commonly carried out, at different scales, in seismology, where it was proved that a larger number of emissions corresponds to smaller amplitudes, whereas larger amplitudes are restricted to few events. Therefore, $N(v)$ can be expressed, with a good approximation, through the constants a and c, according to the Gutenberg-Richter power-law [2]:

$$\log N(v) = c - av \tag{1}$$
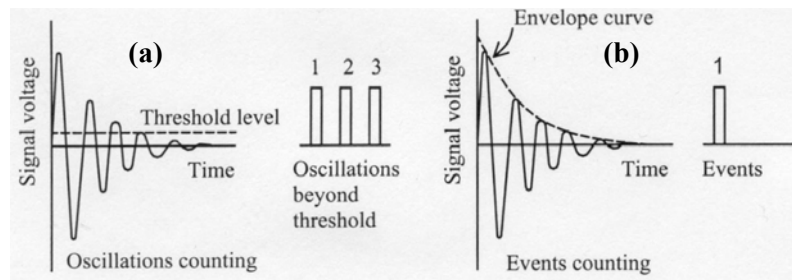
Fig.1 – Detected signals by AE technique

FAILURE MECHANISMS OF CONCRETE IN COMPRESSION

The behavior of concrete elements at rupture is explained by their heterogeneity. Experimental investigations have shown how the nature of the stress-strain curve is related to preexistent internal bond cracks. In synthesis, three aspects seem to influence the concrete failure in compression:
(a) the type of contact, depending on the utilized platens;
(b) the element shape, defined in terms of the ratio between the height h of the specimen and the characteristic size d of its cross-section;
(c) the characteristic specimen size scale d.
In fact, friction, yielded by rigid steel platens, affects the stress field, inducing radial compressive stresses close to the ends; the higher the ratio h/d, the more rapidly these effects vanish far from the ends. This phenomenon implies the transition from crushing to splitting for uniaxially compressed specimens. The global scale-dependent mechanical behavior can be explained by Linear Elastic Fracture

Mechanics (LEFM), which contemplates energy dissipation over fracture surfaces. As is well-known, the nominal stress at failure varies as $d^{-1/2}$ for all the LEFM solutions, so that 1/2 turns out to be the slope of the strength versus size decrease in a bilogarithmic diagram [7,8]. The most dangerous defect proves to be of a size proportional to the structural dimension and this corresponds to very disordered materials. In the case of less random materials, the slope is lower than the absolute value of the power of the LEFM stress-singularity and vanishes for perfectly ordered materials.

EXPERIMENTAL SETUP

Test specimens and testing equipment

As pointed out in the Introduction, all the cylinders were obtained by drilling from a concrete wall. The concrete, of poor mechanical characteristics, has an apparent specific weight of about 2.23 g/cm^3 and a maximum aggregate size of about 15 mm. The cement amount is not over 100 kg/m^3. Three different diameters are considered in a maximum scale range 1:3.6. The specimens present a height/diameter ratio h/d=1 and d is chosen equal to 27.5, 59, 99 mm, respectively. Six identical specimens have been tested for d=99 and 59 mm, and three identical specimens for d=27.5 mm. The geometries of the tested specimens are presented in Fig.2. In Table 1 the average values obtained from the experiments are reported.

The tests have been performed by a MTS machine (810 model) with a capacity of 250 kN. This kind of machine is controlled by an electronic closed-loop servo-hydraulic system. It is therefore possible performing tests under load or displacement control. The displacements are recorded by a couple of inductive-bridge transducers (HBM W10 model) applied on the loading platens, with a maximum stroke of 10mm.
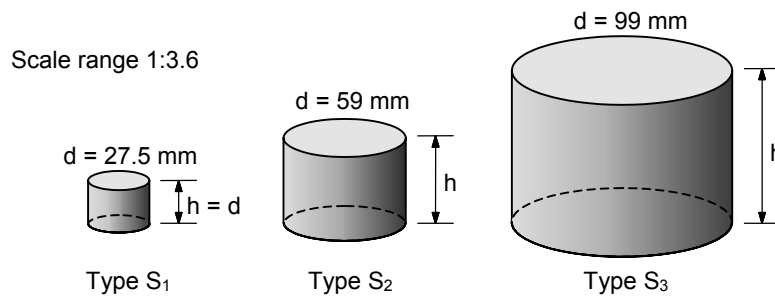
Fig.2 – Geometries of the tested specimens

Specimen type	Diameter (mm)	Peak load (daN)	Stress at peak load σ_u (Mpa)	Stress-Strain Area up to ε=0.05 (Mpa)	N_T number at ε=0.05	N_T/Vol. at ε=0.05
S1	27.5	451.4	7.6	0.216	2500	0.153
S2	59	1941.2	7.1	0.181	7000	0.043
S3	99	5003.5	6.5	0.167	9500	0.012

Tab.1 – Average values obtained from experiments

Displacement control and boundary conditions. All compression tests have been performed under displacement control, by imposing a constant rate of the displacement of the upper loading platen. We adopted a displacement rate equal to 4×10^{-4} mm/s for all specimens, in order to obtain a very slow-crack growth and to detect all possible AE signals. In this way, we were able to capture also the softening branch of the stress-strain diagrams.

The system adopted in the compression test utilizes rigid steel platens, the lateral deformation of concrete being therefore confined to the specimen ends, which are forced to have the some lateral deformation as the rigid platens. In this case, shear-stresses develop between specimen and loading platen, causing a three dimensional state of stress at the specimen ends. Therefore, the kind of rupture is likely an oblique shear failure (Fig.3).

AE data acquisition system. The apparatus consists of two piezo-electric transducers (PZT), applied on the specimen surface and calibrated in the frequency range between 100 and 300 kHz, and of two data acquisition systems [1]. The threshold level of the signal is set equal to 100 µV and is amplified up to 100 mV. The amplification gain can be related to the ratio between the output and the input voltage (E_u/E_i), according to the formula $dB=20\log_{10}E_u/E_i$. In the present case, the increment is equal to 60 dB. According to the literature, this represents the typical value used for AE measurements in concrete [3,6]. The oscillation counting capacity has been set equal to 255 counts in 120 seconds, i.e., a single "*event*" is the result of 2 recorded minutes. By means of this system, the intensity of a single event is calculated assuming that the amplitude v of the signals is proportional to the number of counts N_T recorded in the time interval (Event-Counting). Clearly, this hypothesis is fully justified in the presence of slow-crack growth.
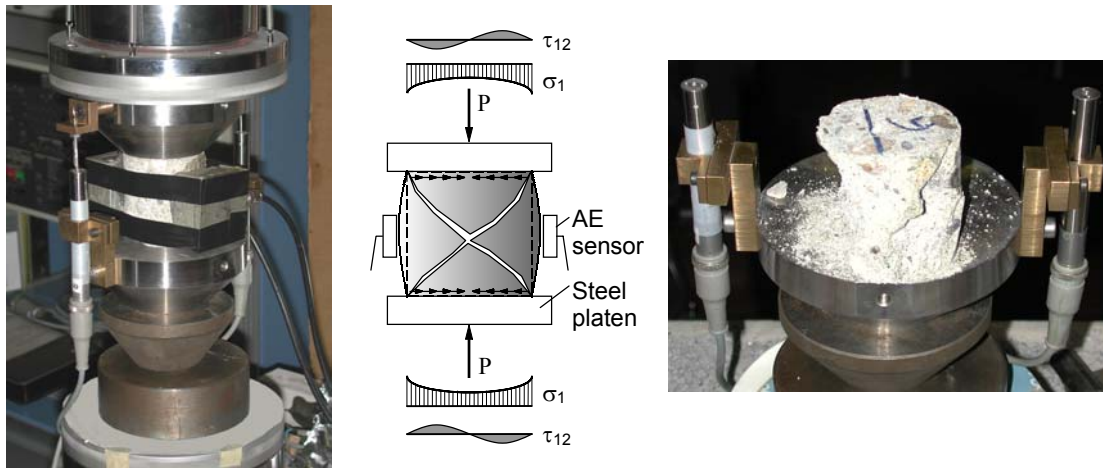
Fig.3 – Apparatus adopted for compression tests and typical shear failure of a concrete specimen

TYPICAL AE EVENT OCCURENCE AND ACTIVITY

The stress versus time curve for a specimen of medium size is represented in Fig.4, as well as similar results can be observed in the other cases. Compressive stress, cumulated event number N_T, and event rate (per each couple of minutes) are depicted in Fig.4a. Fig.4b shows compressive stress and cumulated event number as functions of nominal strain. In the same diagram, the derivative of the cumulative curve is also reported. The cumulative distribution has been determined using, for the sake of simplicity, a standard two parameter exponential function:

$$\widetilde{N}_T = a(1 - e^{b\varepsilon^2}) \tag{2}$$

Parameter a represents the horizontal asymptote of the distribution, while b is obtained imposing that the N_T value in correspondence of the peak-load, σ_u, coincides with the experimental value.
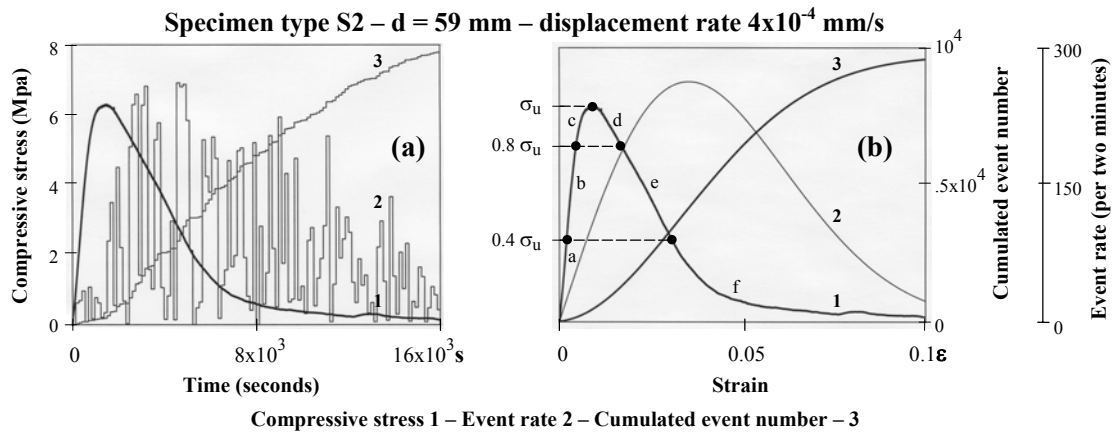
Fig.4 – Compressive stress and AE signals as functions of time or strain

In Fig.4b, the AE data are divided into six regimes according to the stress level (loading stages), from (a) to (f), for the convenience of analysis. The compressive stress is calculated from the imposed compressive load divided by the original cross-sectional area. The nominal strain is the elongation, measured by the control HBM, and divided by the original height of the specimen.

In regime (a), which is the initial portion of the stress-strain curve, few AE events can be recorded because the stress level is rather low at this loading stage. After that, a sensible AE activity starts to be detectable around 42-45% of the peak stress (σ_u), in regime (b), where the stress level is within the interval 0.4-0.8σ_u. In this regime, a small but gradually increasing number of AE events can be recorded, although the material is still deformed elastically. Such a gradually increasing amount of AE events extends to regime (c), in which the stress level varies from 0.8 σ_u to σ_u and the stress-strain response is nonlinear.

The event rate reaches its maximum value at the beginning of regime (f), in the softening branch of the diagram, where the compressive stress is around 0.4σ_u. This

remark implies that the AE activity is closely related to this loading stage, where the central portion of the specimen undergoes extensive cracking that dominates the emission.

SIZE EFFECTS DETECTED BY AE TECHNIQUE

Nominal compressive strength and homogeneity

If we consider the relationship between nominal peak stress (Table 1) and related dimension in logarithmic form [7]:

$$\log \sigma_u = \log \sigma_u(1) - d_\sigma \log d \tag{3}$$

we obtain the function:

$$y = 1.05 - 0.12x. \tag{4}$$

In eq. (3) the slope of the strength decrease, $d_\sigma = 0.12$, identifies a rather random material characterized by a reduced size effect. This behavior is frequent in compression tests with rigid steel platens, where the kind of rupture is an oblique share failure [7]. This is confirmed by the power-law represented in eq. (1), from which we obtain:

$$a = c - av - [c - a(v+1)] = \log N(v) - \log N(v+1) = \log \frac{N(v)}{N(v+1)}. \tag{5}$$

Increasing the value of a, the number of events with low energy increases with respect to the number of events with high energy. This parameter can be therefore used to characterise the homogeneity of the material undergoing damage. The cumulative distribution functions for three specimens of different sizes are represented in Fig.5. These functions have been obtained by calibrating the parameters of eq. (1) with the extreme values of the experimental distribution. The minimum value $N(v)=1$ corresponds to the highest intensity of the events that the instruments can record, i.e., to $v_{max}=255$:

$$c - av_{max} = \log N(v_{max}) = \log 1 = 0. \tag{6}$$

This also implies that $v_{max}=c/a=255$. Notice that, according to the original approach by Richter [2], we preferred to interpret the experimental data by means of the extreme values instead of using a nonlinear best-fit procedure. As we observe in the graphs of Fig.5, for the three tested specimen sizes the parameter a is in inverse proportion to size. This exhibits the greater homogeneity of the smallest size specimen ($d=27.5$mm) with respect to the largest size one ($d=99$mm). On the other hand, the limited dispersion of diagram values confirms that the material is characterised by a low statistical dispersion.
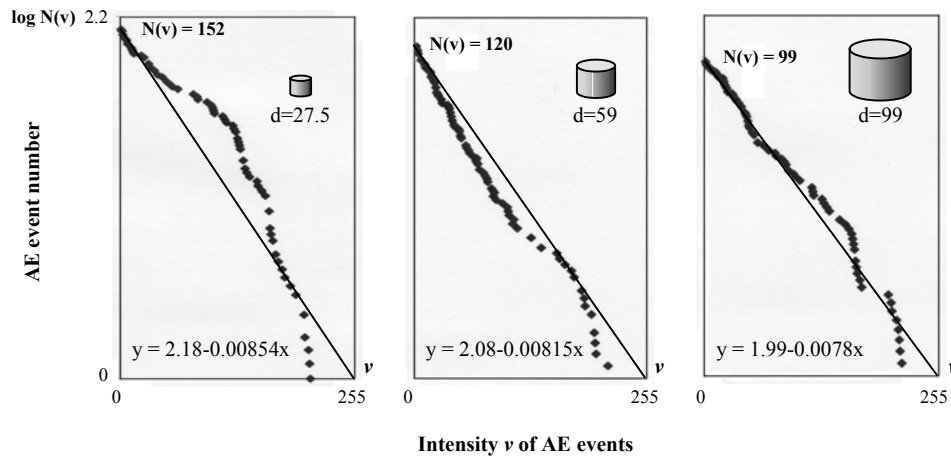
Fig.5 – Cumulative distribution function of AE events

Dissipated energy density

The performed compression tests show a decrease in dissipated energy density with increasing specimen dimension. For all the tested specimens, the dissipated energy density E_r has been evaluated by considering the area under the stress-strain curve up to $\varepsilon = 0.05$. This is equivalent to consider the area under the P-δ curve divided by the volume of the specimen. The average values of these areas are reported in Table 1. In the same table are also reported the cumulated event number N_T density, represented by the ratio of N_T to the specimens volume (N_T/V).
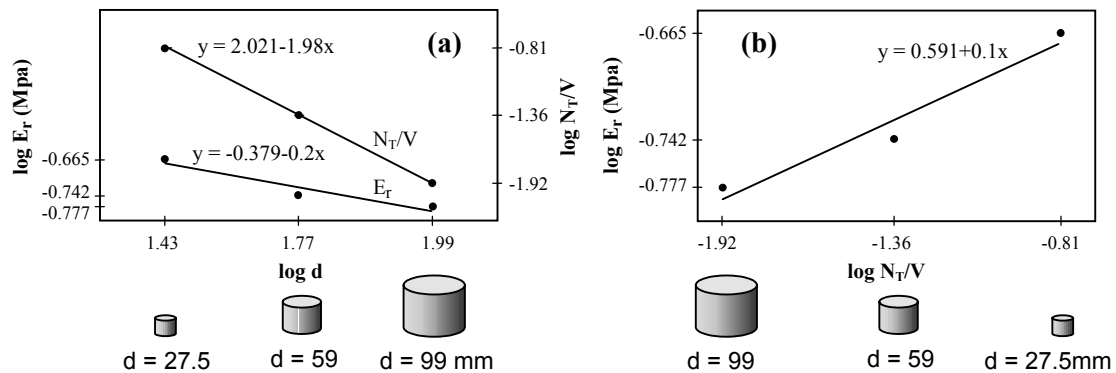
Fig.6 – Size effects on dissipated energy density

Plotting E_r and N_T/V versus specimen size, in logarithmic form, the trend is a decrease by increasing specimen size (Fig.6a). This is not a peculiarity of the material and can be interpreted by considering the fragmentation and comminution theories [9], according to which the slope 0.2 of energy decrease identifies a failure process like crashing, where the energy dissipation occurs tendentially in the material volume. The decrease of the released energy is also well in accordance with the N_T/V trend, even though with emphasized slope in the latter case.

On the other hand, connecting in a bi-logarithmic plane the values of N_T/V and E_r (Fig.6b) we obtain the function:

$$\log E_r = c + b \log N_T / V ,\qquad (7)$$

that joins the dissipated energy with cumulated event number density during the compression tests.

CONCLUSIONS

By utilizing the AE technique and employing scaling laws well-known in seismology, we have estimated the material homogeneity and the amount of energy released during the fracture process of concrete specimens. With this methodology, it is possible to evaluate the criticality of the loading process, also in larger structural elements, monitoring the nonlinear behavior and detecting the growth of meso-defects and macro-cracks.

AKNOWLEDGEMENTS

REFERENCES

[1] A. Carpinteri, G. Lacidogna, "Monitoring a masonry building of the 18th century by the acoustic emission technique", Proc. of STREMAH VII, Bologna, Ed. WIT Press Southampton, 2001, 327-337.

[2] C.F. Richter, *Elementary Seismology*, W.H. Freeman and Company, San Francisco and London, 1958.

[3] M. Ohtsu, "The history and development of acoustic emission in concrete engineering", *Magazine of Concrete Research*, **48**, 1996, 321-330.

[4] A.A. Pollock, "Acoustic emission-2: acoustic emission amplitudes", *Non-Destructive Testing*, **6**, 1973, 264-269.

[5] B.J. Brindley, J. Holt, I.G. Palmer, "Acoustic emission-3: the use of ring-down counting", *Non Destructive Testing*, **6**, 1973, 299-306.

[6] P. Shah, L. Zongjin, "Localization of microcracking in concrete under uniaxial tension", *ACI Materials Journal*, **91**, 1994, 372-381.

[7] A. Carpinteri, G. Ferro, I. Monetto, "Scale effects in uniaxially compressed concrete specimens", *Magazine of Concrete Research*, **51**, 1999, 217-225.

[8] A. Carpinteri, F. Ciola, N. Pugno, "Boundary element method for the strain-softening response of quasi-brittle materials in compression", *Computers & Structures*, **79**, 2001, 389-401.

[9] A. Carpinteri, N. Pugno, "Fractal and multifractal fragmentation theory for size effects of quasi-brittle materials in compression", *Theoretical and Applied Fracture Mechanics*, 2001, in print.